PROCEEDINGS OF SCIENCE

Continuum limit of generalized charm susceptibilities

Sipaz Sharma[a,*]

[a] *Physik Department, Technische Universität München,*
James-Franck-Straße 1, D-85748 Garching b. München, Germany

E-mail: sipaz.sharma@tum.de

We investigate in detail the sensitivity of the fourth-order charm fluctuation, calculated on the lattice, to the input bare charm quark mass. We approach its continuum limit by employing four different lines of constant physics. We quantify the cutoff effects arising due to bare charm quark mass for both coarser and finer lattices. Finally, we show that the ratios of generalized charm susceptibilities, calculated on coarser lattices, and the continuum-extrapolated fourth-order charm fluctuation are sufficient to obtain the continuum limit of all physical observables relevant to open charm physics.

The 41st International Symposium on Lattice Field Theory (LATTICE2024)
28 July - 3 August 2024
Liverpool, UK

[1]For the HotQCD Collaboration.
*Speaker

PoS(LATTICE2024)192

1. Introduction

Generalized charm susceptibilities are a powerful tool for probing the nature of charm degrees of freedom at finite temperature, T, using lattice QCD techniques. These are derivatives of the QCD pressure, P, with respect to chemical potentials corresponding to the conserved charges: baryon number (B), electric charge (Q), strangeness (S) and charm (C),

$$\chi^{BQSC}_{klmn} = \frac{\partial^{(k+l+m+n)} \ [P\ (\hat{\mu}_B, \hat{\mu}_Q, \hat{\mu}_S, \hat{\mu}_C)\ /T^4]}{\partial \hat{\mu}_B^k \ \partial \hat{\mu}_Q^l \ \partial \hat{\mu}_S^m \ \partial \hat{\mu}_C^n}\bigg|_{\vec{\mu}=0}. \tag{1}$$

Here, we introduce a dimensionless notation for chemical potentials, $\hat{\mu}_X = \mu_X/T$, with $X \in \{B, Q, S, C\}$. Our previous works [1–5] have established that below chiral crossover temperature, $T_{pc} = 156.5 \pm 1.5$ MeV [6], hadrons are the carriers of the charm quantum number, C, whereas at T_{pc} charm deconfinement sets in leading to the emergence of charm quarks as new degrees of freedom. However, the disappearance of charmed hadrons is gradual, and charm quarks give dominant contribution to the partial charm pressure only above 175 MeV. Additionally, lattice investigations of charm susceptibilities have also predicted the existence of experimentally unobserved charmed hadrons in the low temperature phase [2, 7]. As pointed out in one of our previous articles, [5], above conclusions are based on the analysis of the ratios of various linear combinations of the generalized charm susceptibilities. These linear combinations are determined by the relevant physics which one aims to probe. These ratios were calculated on coarser lattices (temporal lattice extent, $N_\tau = 8$) but the conclusions driven from their analysis hold in the continuum limit because the dominant cutoff effects present due to a relatively heavier charm quark mass cancel in the ratios. However, ratios alone are not sufficient to fully understand charm thermodynamics. Therefore, taking the continuum limit of the proxies for the partial pressures of the relevant charm degrees of freedom is crucial. These proxies are constructed from linear combinations of various generalized charm susceptibilities. In the next sections, a summary of the approach to continuum limit of the least noisy charm susceptibility ($\chi^{BQSC}_{0004} \equiv \chi^C_4$) is provided – full details will be provided in our forthcoming publication. We argue that only continuum extrapolated χ^C_4 is enough to convert observables, which are normalized by χ^C_4 and computed on coarser lattices, to their absolute continuum values.

2. Lattice setup

We used (2+1)-flavor HotQCD configurations generated using HISQ action and a Symanzik-improved gauge action for physical strange-to-light quark mass ratio, $m_s/m_l = 27$, for three temporal lattice extents, $N_\tau = 8$, 12 and 16. The calculation of derivatives of the QCD pressure was achieved by the unbiased stochastic estimation of various traces using random noise method. In particular, 500 random vectors were used to calculate traces relevant for χ^C_4 on each configuration. The temperature scale was determined using a parametrization of the kaon decay constant in lattice units, af_K, as given in [8], and the conversion to physical units was performed using the f_K value given in the latest FLAG review [9]. Since the temperature is given by $T = (aN_\tau)^{-1}$, this implies that we used three different lattice spacings at a fixed temperature.

We treated charm quark in the quenched approximation, and used the so-called epsilon term to remove $O((am_c)^4)$ tree-level lattice artifacts [10]. In order to understand the cutoff effects in

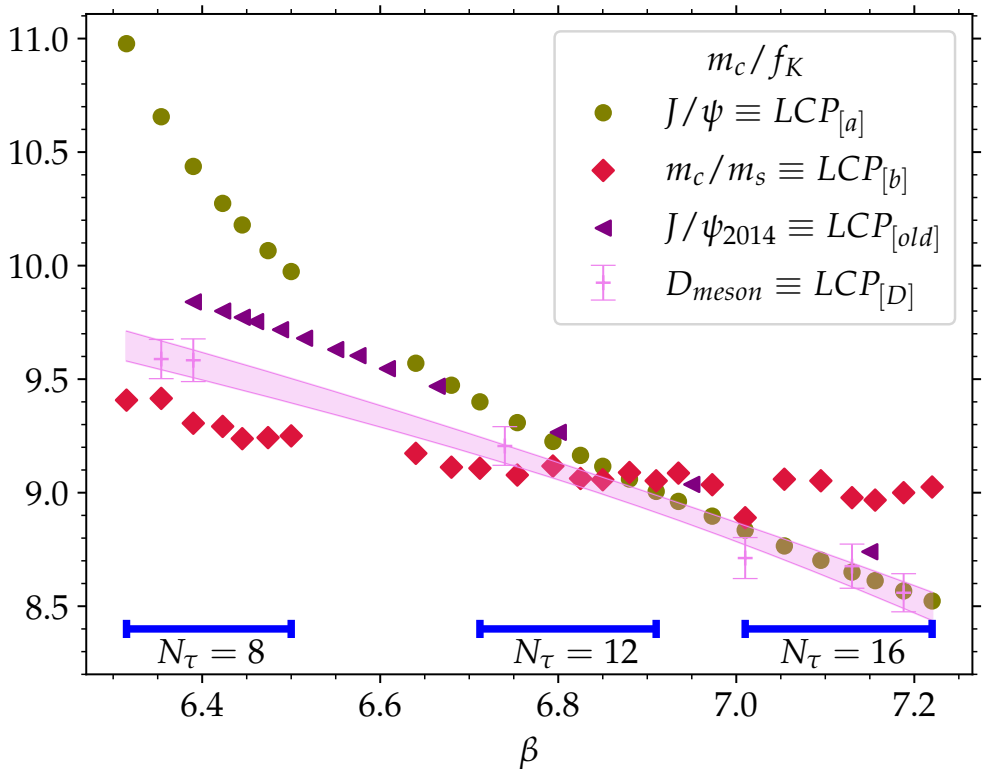

Figure 1: Shown are the bare charm quark mass values normalised by af_K as a function of the inverse gauge coupling, β, tuned using four different criteria to define lines of constant physics: $\text{LCP}_{[a]}$, $\text{LCP}_{[b]}$, $\text{LCP}_{[old]}$, and $\text{LCP}_{[D]}$ (see text for definitions). The band shows bootstrap error of $\text{LCP}_{[D]}$ values. The blue lines explicitly show the ranges of inverse gauge couplings, β, relevant for three different temporal lattice extents used in this work.

χ_4^C due to input bare charm quark mass, am_c, we used am_c values tuned on four different Lines of Constant Physics (LCPs) shown in Fig. 1 as functions of the inverse gauge coupling, β:

• $\text{LCP}_{[a]}$ was tuned by keeping spin-averaged charmonium mass fixed to its physical value. For further details, see [1].

• $\text{LCP}_{[b]}$ was tuned by keeping the ratio am_c/am_s fixed to its Particle Data Group (PDG) value, 11.76 [11]. This LCP is based on a strange quark mass tuned by fixing the mass of the fictitious pseudoscalar meson, $\eta_{s\bar{s}}$, to 695 MeV [12]. However, this is slightly higher than the value given by χPT, 686 MeV, indicating that the strange quark mass is 2.6% larger than its physical value. In addition to this, for finer lattices corresponding to $\beta > 7.03$, the resulting lattice mass of $\eta_{s\bar{s}}$ is larger than 695 MeV by about 3.5%. This drift from 695 MeV was further corrected by using lowest order χPT such that $M^2_{\eta_{s\bar{s}}} \propto m_s$ (see Ref. [13]) but the configuration generation did not take into account this corrected version of LCP. This mistuning is clearly reflected in the am_c values corresponding to $\text{LCP}_{[b]}$ in the higher β range of Fig. 1.

• $\text{LCP}_{[old]}$ is an older prescription used in Ref. [7]. It also was tuned by keeping spin-averaged charmonium mass fixed to its physical value.

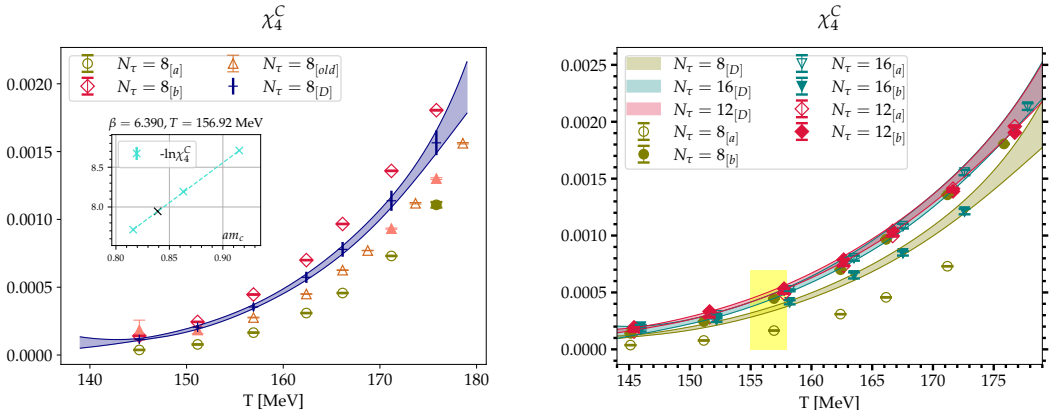

Figure 2: Shown is χ_4^C as a function of temperature constructed on LCP$_{[D]}$ using its calculated values on LCP$_{[a]}$, LCP$_{[b]}$ and LCP$_{[old]}$ for $N_\tau = 8$ lattices. The solid points and the bands shown are results of [2, 2] Padé interpolations. The inset shows linear interpolation of $-\ln \chi_4^C$ in am_c at $\beta = 6.390$ and the black cross represents $-\ln \chi_4^C$ on LCP$_{[D]}$*(Left)*. Lattice QCD results for χ_4^C for different values of the temporal lattice extents calculated on the two different LCPs, *i.e.* LCP$_{[a]}$ and LCP$_{[b]}$, and constructed on LCP$_{[D]}$. χ_4^C for $N_\tau = 16$ on LCP$_{[D]}$ represents our continuum estimate. The yellow band represents T_{pc} with its uncertainty *(Right)*.

• am_c values on LCP$_{[D]}$ correspond to physical D-meson mass. am_c parametrization on this LCP will be given in our forthcoming publication.
In the following, results based on above LCPs will carry subscripts $[a]$,$[b]$,$[old]$ and $[D]$ respectively.

3. Fourth-order charm fluctuation on different LCPs

In the hadron gas phase below T_{pc}, at a temperature, T, contribution to the partial charm pressure from each charmed state of mass, m_i carrying quantum numbers, B_i, Q_i,S_i, C_i, is proportional to,

$$\left(\frac{m_i}{T}\right)^{3/2} e^{-m_i/T} \; [1 + \mathbb{O}((m_i/T)^{-1})]\cosh(B_i\hat{\mu}_B + Q_i\hat{\mu}_Q + S_i\hat{\mu}_S + C_i\hat{\mu}_C). \tag{2}$$

This also holds true in the QGP phase where charm quarks and charmed hadrons coexist [2]. Therefore, the exponential suppression in (2) dictates that the lightest charmed state should give the dominant contribution to the partial charm pressure. In the hadron gas phase, the lighest charmed state is D-meson. In the QGP phase, slightly above T_{pc}, thermal mass of charm quark-like quasi particle is around D-meson mass [5]. Therefore, based on thermodynamical arguments, χ_4^C on LCP$_{[D]}$ will be closer to the physical case, particularly at relatively coarser $N_\tau = 8$ lattices. As can be inferred from Fig. 1, am_c at the lowest β value, 6.315, used in the calculation of χ_4^C at $N_\tau = 8$, varies by 16 % between LCP$_{[a]}$ and LCP$_{[b]}$, whereas for the lowest β value of $N_\tau = 12$ calculation, 6.712, this variation reduces to 3%. However, as discussed in the previous section, due to mistuning of am_s, LCP$_{[b]}$ drifts away from LCP$_{[a]}$ for $\beta > 6.9$. Nonetheless, LCP$_{[a]}$ and LCP$_{[D]}$ converge in the higher β range, which is relevant for the finest $N_\tau = 16$ lattices.

The mass of lightest charmed state is proportional to am_c, and since charm quark mass is an order of magnitude larger than the temperature of interest, thus even a small change in the charm

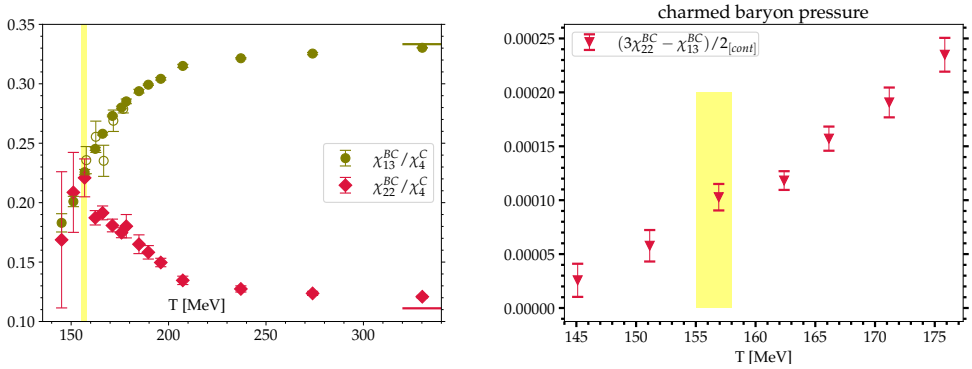

Figure 3: The ratios χ_{mn}^{BC}/χ_4^C as function of the temperature compared to the ideal quark gas predictions at high temperatures shown as horizontal lines. Solid markers represent $N_\tau = 8_{[b]}$ results, whereas unfilled markers of the same color represent the respective $N_\tau = 12_{[b]}$ results. Solid markers for $T > 176$ MeV represent $N_\tau = 8_{[old]}$ results taken from Ref. [7]. The vertical yellow band represents chiral crossover temperature with its uncertainty *(Left)*. Shown is the continuum result of a proxy for charmed baryon partial pressure as function of temperature. The vertical yellow band represents chiral crossover temperature with its uncertainty *(Right)*.

quark mass can lead to large changes in the Boltzmann weight in (2). This sensitivity of the partial charm pressure to am_c is clearly reflected in its fourth derivative w.r.t. $\hat{\mu}_C$ shown in Fig. 2 [Left] for $N_\tau = 8$ lattices. For $N_\tau = 8$, we used lattice calculations of χ_4^C on three LCPs: LCP$_{[a]}$, LCP$_{[b]}$, LCP$_{[old]}$ to construct χ_4^C on LCP$_{[D]}$. As shown in the inset of Fig. 2 [Left] , at each temperature, we linearly interpolated $-\ln \chi_4^C$ in am_c to obtain χ_4^C on LCP$_{[D]}$. Similarly, we constructed χ_4^C on LCP$_{[D]}$ for $N_\tau = 12$ and 16. Futher details, especially on error analysis, will be given in a forthcoming publication.

4. Continuum limit

We show lattices calculations of χ_4^C on LCP$_{[a]}$ and LCP$_{[b]}$ for three N_τ values in Fig. 2 [Right]. The figure also shows χ_4^C constructed on LCP$_{[D]}$ for three N_τ values. As expected, with the convergence of am_c on LCP$_{[a]}$ and LCP$_{[D]}$, χ_4^C also converges on LCP$_{[a]}$ and LCP$_{[D]}$ for $N_\tau > 8$. As can be seen from Fig. 2 [Right], the χ_4^C bands corresponding to LCP$_{[D]}$ agree within errors for $N_\tau = 12$ and 16. Therefore, we use $N_\tau = 16$ result as our continuum estimate of χ_4^C.

It was shown in our previous work [2] that at a fixed N_τ, sensitivity to the choice of LCP cancels to a large extent in the ratios of generalized susceptibilities. In Fig. 3 [Left], two $N_\tau = 8$ baryon-charm correlations normalised by χ_4^C are shown. Additionally, agreement of $N_\tau = 8_{[b]}$ and $N_\tau = 12_{[b]}$ results of χ_{13}^{BC}/χ_4^C in Fig. 3 [Left] implies that the cutoff effects cancel to a large extent in the ratios. Therefore, physical conclusions drawn from ratios calculated on the coarser lattices hold in the continuum limit. This implies that by multiplying $N_\tau = 8_{[b]}$ version of observables normalised by χ_4^C to the continuum version of χ_4^C and after doing error propagation, one can obtain continuum limit of the relevant observables. Fig. 3 [Right] shows a linear combination of the unnormalised versions of baryon-charm correlations of Fig. 3 [Left]. According to the quasi-particle model from Ref. [2], $(3\chi_{22}^{BC} - \chi_{13}^{BC})/2$ is a proxy for the charmed baryon pressure, and

Fig. 3 [Right] shows its continuum result. Similarly, continuum limit of other physical quantities can also be obtained by following above procedure.

5. Conclusions and Summary

We showed that the generalized charm susceptibilities are sensitive to the choice of LCPs used to tune the bare charm quark mass. In order to reduce cutoff effects for coarser lattices at finite temperature, the choice of LCP should be motivated by the thermodynamics. On the other hand, for finer lattices, correctly tuned LCPs converge. By quantifying the cutoff effects arising due to bare charm quark mass in the fourth-order charm fluctuation, we obtained its continuum limit. Finally, using the continuum extrapolated χ_4^C, we indirectly obtained continuum results of other physical quantities essential for describing charm thermodynamics. As an example, we showed continuum extrapolated charmed baryon pressure.

Acknowledgments

This work was supported by The Deutsche Forschungsgemeinschaft (DFG, German Research Foundation) - Project number 315477589-TRR 211, "Strong interaction matter under extreme conditions". The authors gratefully acknowledge the computing time and support provided to them on the high-performance computer Noctua 2 at the NHR Center PC2 under the project name: hpc-prf-cfpd. These are funded by the Federal Ministry of Education and Research and the state governments participating on the basis of the resolutions of the GWK for the national high-performance computing at universities (www.nhr-verein.de/unsere-partner). Numerical calculations have also been performed on the GPU-cluster at Bielefeld University, Germany. We thank the Bielefeld HPC.NRW team for their support.

All computations in this work were performed using `SIMULATeQCD` code [14]. All the HRG calculations were performed using the AnalysisToolbox code developed by the HotQCD Collaboration [15].

References

[1] S. Sharma, *Charm fluctuations in (2+1)-flavor QCD at high temperature*, *PoS* **LATTICE2022** (2023) 191 [2212.11148].

[2] A. Bazavov, D. Bollweg, O. Kaczmarek, F. Karsch, S. Mukherjee, P. Petreczky et al., *Charm degrees of freedom in hot matter from lattice QCD*, *Phys. Lett. B* **850** (2024) 138520 [2312.12857].

[3] HotQCD collaboration, *Charm Fluctuations and Deconfinement*, *POS* **LATTICE2023** (2024) 200 [2401.01194].

[4] S. Sharma, *Persistence of charmed hadrons in QGP from lattice QCD*, *to appear in Int. J. Mod. Phys. A* **40** (2025) [2410.04222].

[5] S. Sharma, F. Karsch and P. Petreczky, *Thermodynamics of charmed hadrons across chiral crossover from lattice QCD*, *J. Subatomic Part. Cosmol.* **3** (2025) 100044 [2501.01300].

[6] HotQCD collaboration, *Chiral crossover in QCD at zero and non-zero chemical potentials*, *Phys. Lett. B* **795** (2019) 15 [1812.08235].

[7] A. Bazavov et al., *The melting and abundance of open charm hadrons*, *Phys. Lett. B* **737** (2014) 210 [1404.4043].

[8] HotQCD collaboration, *Second order cumulants of conserved charge fluctuations revisited: Vanishing chemical potentials*, *Phys. Rev. D* **104** (2021) [2107.10011].

[9] Flavour Lattice Averaging Group (FLAG) collaboration, *FLAG Review 2024*, 2411.04268.

[10] HPQCD, UKQCD collaboration, *Highly improved staggered quarks on the lattice, with applications to charm physics*, *Phys. Rev. D* **75** (2007) 054502 [hep-lat/0610092].

[11] Particle Data Group collaboration, *Review of particle physics*, *Phys. Rev. D* **110** (2024) 030001.

[12] A. Bazavov et al., *The chiral and deconfinement aspects of the QCD transition*, *Phys. Rev. D* **85** (2012) 054503 [1111.1710].

[13] HotQCD collaboration, *Equation of state in (2+1)-flavor QCD*, *Phys. Rev. D* **90** (2014) 094503 [1407.6387].

[14] HotQCD collaboration, *SIMULATeQCD: A simple multi-GPU lattice code for QCD calculations*, *Comput. Phys. Commun.* **300** (2024) 109164 [2306.01098].

[15] D.A. Clarke, L. Altenkort, J. Goswami and H. Sandmeyer, *Streamlined data analysis in Python*, *PoS* **LATTICE2023** (2024) 136 [2308.06652].

PoS(LATTICE2024)192